



Aluminum Oxide Nanoparticles (Al_2O_3 -Nps) Toxicity in Sprague-Dawley Rats: Pathological Investigations.

Amira E. Shehata¹; Dina A. Mahrous²; Hamed Saleh³; Wael M. Goda¹; Shahenaz M. H. Hassan⁴; Yasser S. El-Sayed³; Abou-rawash A. A.^{*1}; Hoda A. Abdellatif¹.

¹ Pathology department, Faculty of Veterinary Medicine, Damanhour University, Egypt.

² Clinical pathology department, Faculty of Veterinary Medicine, Damanhour University, Egypt.

³ Forensic Medicine & toxicology department, Faculty of Veterinary Medicine, Damanhour University, Egypt.

⁴ Alexandria Regional Laboratory, Animal Health Research Institute (AHRI), Agriculture Research Center (ARC), Egypt.

Abstract: Nanoparticles (NPs), particularly aluminum oxide (Al_2O_3 -NPs), are commonly utilized across various sectors, including industrial and biomedical applications, healthcare, cosmetics, and food production. The experimental animals (n = 30 male Sprague Dawley rats) were divided into the following groups: the negative control (NC); G1 (15 mg/kg Bw Al_2O_3 -NPs) and G2 (30 mg/kg Bw Al_2O_3 -NPs) were randomly assigned to three groups (10 rats in each group). The study revealed that rats exposed to Al_2O_3 -NPs showed non-significant differences in initial body weight, final weight, weight gain, and relative liver and kidney weight. Malondialdehyde (marker lipid of peroxidation) level was significantly ($P \leq 0.05$) increased in the liver and renal tissues. Pathological alterations in liver tissues included focal degeneration of hepatocytes and necrosis with changes in the portal areas. The kidney tissues displayed focal interstitial nephritis, degeneration, and necrosis in renal tubular epithelium. This study used a variety of pathological studies to determine the toxicological effect of Al_2O_3 -NPs in vivo.

Keywords: Nanoparticle; Aluminum oxide; Liver; Kidney; Pathology; Oxidative stress

*Correspondence: **Abou-rawash A. A.**

Pathology Department, Faculty of Veterinary Medicine, Damanhour University, Damanhour-22511, El-Beheira, Egypt

Email: Rawashaa@yahoo.com

P ISSN: 2636-3003

EISSN: 2636-2996

DOI: 10.21608/djvs.2025.345435.1145

Received: December 23, 2024; Received in revised form: January 25,

2025; accepted: June 20, 2025

Editor-in-Chief:

Ass. Prof /Abdelwahab A. Alsenosy (editor@vetmed.dmu.edu.eg)

1. Introduction

Nanoparticles (NPs) are indeed fascinating materials with unique properties that have revolutionized various fields. they are defined as particles with dimensions ranging from 1 to 100 nanometers (Lee & Jun, 2019). NPs can exist in various forms, including amorphous, polycrystalline, dense, porous, or hollow structures. Their nanoscale dimensions result in properties that differ substantially from bulk materials of the same composition (Abd-Elhakim et al., 2021).

The unique characteristics of nanoparticles have led to their widespread use in numerous fields such as medicine because of their antimicrobial, anti-inflammatory, antiviral and anticancer properties. In addition, it is used in agriculture, industry and energy as they are utilized in crop protection and fertilizers and also used for water disinfection. Furthermore, they are incorporated into various personal care products as cosmetics, food processing and packaging, food supplements, textiles, fuel, water disinfection and activated carbon filters (M. I. Yousef, T. F. Mutar, & M. A. E.-N. Kamel, 2019).

Metal-based NPs have attracted considerable interest in recent years due to their distinctive properties, including a **high surface area**, **optical activity**, **mechanical strength**, and **chemical reactivity**. These attributes make them particularly valuable for a range of **biomedical applications**, especially in addressing complex diseases such as cancers, intricate infections, and autoimmune disorders (Kalashnikova et al., 2020; Rashki et al., 2021; Shin et al., 2018).

Despite their remarkable properties, the use of nanoparticles raises some concerns: as their small size allows them to interact with biological systems in ways that larger particles cannot potentially leading to unintended effects. As the dose increases, nanoparticles can become toxic due to their enhanced uptake by tissues. It also has many environmental impact which still representing an area of ongoing research

(Awashra & Mlynarz, 2023; Li & Tang, 2020).

Al₂O₃-NPs have unique properties that make them valuable in various fields such as medicine, electronics, agriculture, food processing and biotechnology. However, these same properties can also lead to potential toxic effects on human health and the environment. The buildup of nanoparticles in organs can result in various toxic effects, such as oxidative stress, inflammation, and genotoxicity. These effects are influenced by the nanoparticles' size, shape, surface properties, and exposure route (Saratale et al., 2018).

NPs can induce oxidative stress by generating reactive oxygen species (ROS), which can damage cellular components like DNA, proteins, and lipids. This oxidative stress is a common pathway leading to apoptosis, cell damage and death (Kumah et al., 2023).

This investigation explores the crucial characteristics and consequences of administering a dose of 15mg/kg and 30mg/kg body weight (BW) of Al₂O₃-NPs in rat liver and kidney tissues. We analyze how this concentration can adversely affect animal tissues, via induction of hepato-renal toxicity particularly in relation to the induction of cell injury and pathological alterations.

2. Material and methods:

a. The ethical assessment

The research protocol underwent ethical review and approval by the Institutional Animal Care and Use Committee (IACUC) at Damanhur University's Faculty of Veterinary Medicine in Egypt (DMU/VetMed-2024/029). This approval process is essential for ensuring the ethical conduct of animal experiments.

b. Tested compound:

Al₂O₃-NPs (about 50-100nm particle size) purchased from Sigma-Aldrich (St. louis, MO, USA, product number 544833).

c. Characterization of Al₂O₃-NPs:

To examine the physical properties of these nanoparticles at high resolution transmission electron microscope (TEM) was

employed to explore the characteristics of the used NPs. First, aqueous solutions of the Al_2O_3 -NPs were prepared. These solutions were then carefully loaded onto specialized **carbon coated TEM grids** containing 200 mesh. By using TEM, researchers can obtain detailed images of the nanoparticles at the nanoscale. This allows direct visualization and measurement of key characteristics such as; particles size and morphology.

d. **Laboratory animal management and Experimental design:**

Thirty 7-week-old male Sprague Dawley rats ($n=30$), weighing 120 ± 10 g were obtained from the faculty of Agriculture at Alexandria University. The rats were housed in a well-ventilated lab in stainless-steel cages with sterile husk bedding material. Prior to beginning the experiment, the animals underwent a 14-day acclimation period in a controlled environment with a temperature of $24 \pm 2^\circ\text{C}$, humidity of $60 \pm 10\%$, and a 12-hour light-dark cycle. The rats had unrestricted access to water and a pellet diet containing approximately 19% protein.

Following the 15-days adaptation period, the experimental animals were randomly allocated into three groups, with 10 rats in each group: Control: received 0.9% normal saline via intraperitoneal (I.P.) injection. The second group received 15mg/kg BW of Al_2O_3 -NPs and the third group received 30mg/kg BW of Al_2O_3 -NPs via I.P injection for 60d (A. De et al., 2020).

e. **Nanoparticle preparation and Administration:**

Al_2O_3 -NPs were freshly prepared based on the weight of each animal by suspending the NPs in 0.9% normal saline. On the day of injection, the NPs suspensions were vortexed for 10 minutes to ensure thorough mixing and then ultrasonicated for 15 minutes to disperse the nanoparticles and prevent the re-adhesion. The animals were exposed to these NPs via

I.P. injection once every two days for a total of 60 days.

f. **Body weight and clinical signs:**

The body weight of each animal was recorded on the first day following the adaptation period, every week throughout the experiment, and on the day of sample collection. The clinical signs were observed during the experiment.

g. **Sampling:**

At the 60-day post-treatment period, the rats were euthanized using diethyl ether for deep anesthesia. The rats then weighted, and PM examination was proceeded immediately after death. The organs were collected and weighted. Two specimens were then collected from liver and kidney. Suitable specimens of tissues were collected and immediately frozen until used for oxidative stress essay. The other specimens were collected and immediately fixed in 10% neutral buffered formalin for 48hrs.

h. **Histopathological examination:**

Tissues collected from 30 animals ($n=10$) as two specimens from each animal were fixed underwent dehydrated using a graded series of increasing alcohol concentrations. Following dehydration, the tissues were cleared with xylol to remove the alcohol and prepared for paraffin infiltration. The cleared tissues were then embedded in melted paraffin wax maintained at a temperature of 65°C . The paraffin-embedded tissue blocks were sectioned at $3\text{--}5\mu\text{m}$ thickness. The tissue sections were transferred to a water bath set at 45°C to allow them to flatten and expand. The sections were collected on glass slides, cleaned and allowed to dry completely on a hot plate. The tissue sections were deparaffinized using xylol then stained by **Hematoxylin and Eosin (H&E) Staining**. The prepared tissue slides were examined under a light microscope for detailed analysis of the cellular and structural

features (Suvarna, Layton, & Bancroft, 2018).

i. **Oxidative stress assay:**

The oxidative stress biomarkers, including **Malondialdehyde (MDA)**, was measured using liver and kidney homogenates (Biodiagnostics in Cairo, Giza, Egypt) following the established manufacturers protocols (Draper & Hadley, 1990).

2.10. Statical analysis:

The obtained data were statistically analyzed using SPSS version 20 using One Way ANOVA test and $P \leq 0.05$ was considered statistically significant and $P \leq 0.001$ highly significant according to (Murrell, Leighton, Boswell, & Gasbarre, 1989). The values were represented by the letters (a, b and c) as the highest value is (a).

3. Results:

a. TEM analysis of NPs:

The results of shape and dimensions analysis of Al_2O_3 -NPs by using TEM showed distinct differences in their morphological features and sizes. TEM imaging revealed that Al_2O_3 -NPs exhibited a spherical shape under TEM observation. The sizes of Al_2O_3 -NPs were typically less than 50nm (**Fig 1**).

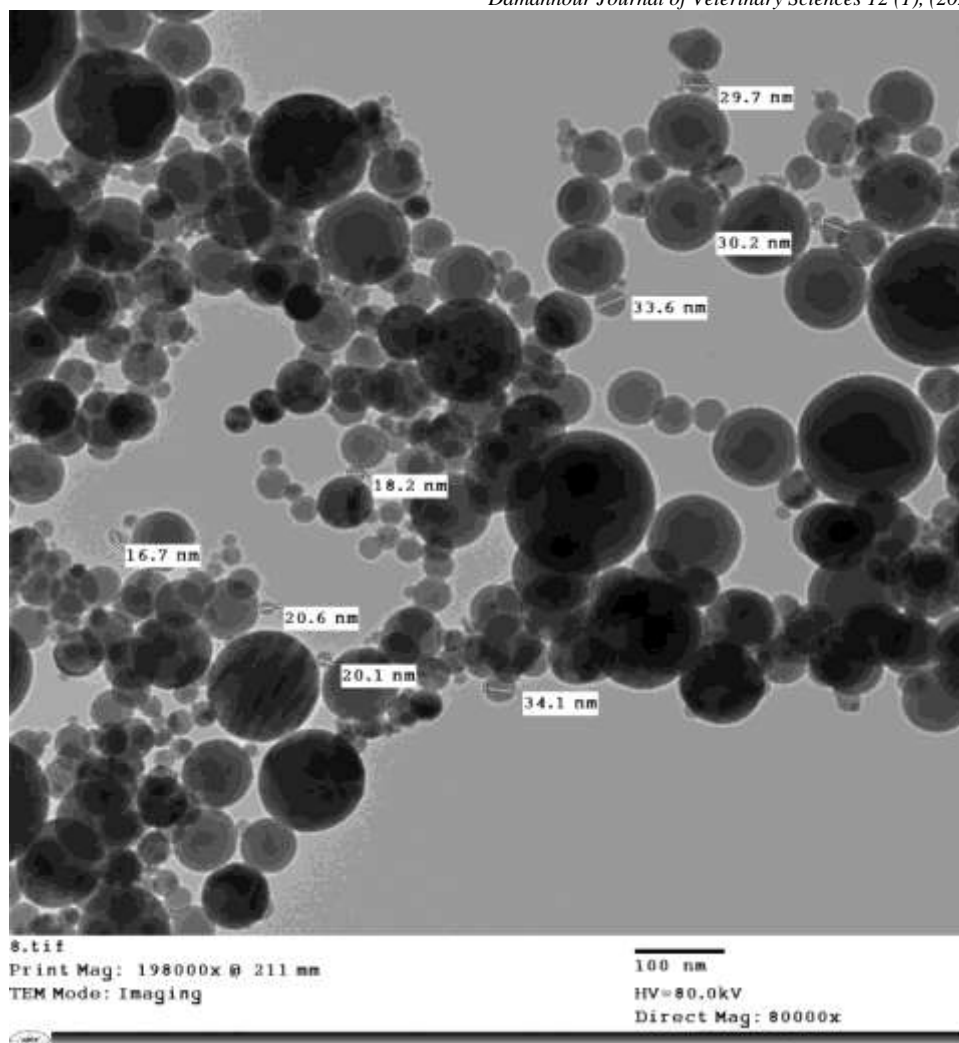


Fig 1: Al₂O₃-NPs characterization with TEM showed the nanoparticles were less than 100nm in diameter with spherical shape as it ranged from 18.2nm to 34.1nm.

1.1.Clinical signs

Most of the treated rats displayed nonspecific clinical signs as; depressive behaviors, indicating potential distress or discomfort associated with the treatment in the majority of the rats.

1.2.Gross pathological finding

The growth pathological features revealed a small pinpoint area of necrosis on kidney and liver tissues of Al₂O₃-NPs when compared to the control group (Fig2).

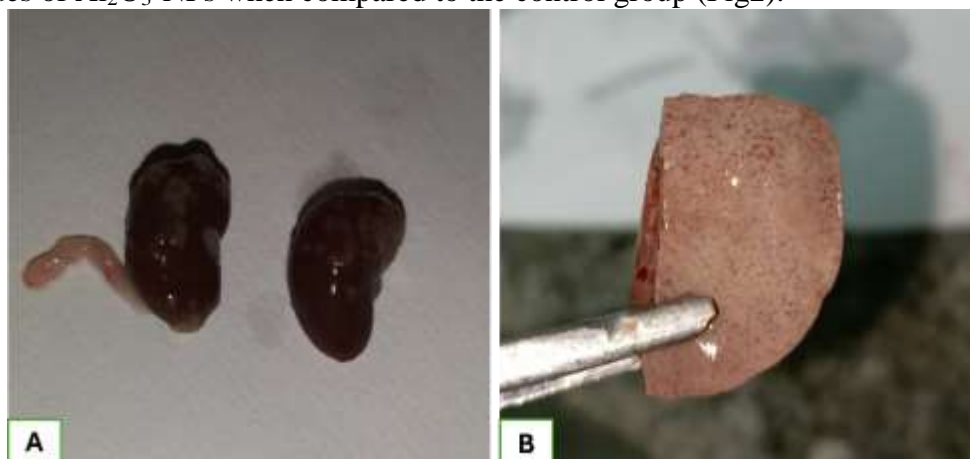


Fig 2: growth pathology of liver and kidney (A): kidney of 15mg/kg Al₂O₃-NPs showed small pinpoint areas of necrosis. (B): liver of 30mg/kg Al₂O₃-NPs showed minute pinpoint area of necrosis.

1.3.Effect of NPs administration on body weight gain and organ weights

The results reveal that there were no statistically significant differences in initial body weight, final weight, weight gain, relative liver and kidney weight between the control group and the treated groups (Table 1).

| Group | Initial weight | Final weigh | Weight gain | Relative liver weight | Relative kidney weight |
|---------|-------------------------|-----------------------|----------------------|------------------------|------------------------|
| Control | 133.3±1.76 ^a | 208±4.05 ^a | 95±5.29 ^a | 3.8±0.233 ^a | 0.67±0.07 ^a |
| Low AL | 115±1.00 ^a | 197±1.15 ^a | 82±2.12 ^a | 3.6±0.012 ^a | 0.63±0.01 ^a |
| High AL | 116±2.18 ^a | 210±3.78 ^a | 93±1.76 ^a | 4.08±0.22 ^a | 0.66±0.06 ^a |

Table 1: Data presented as Mean ± SE. This data was analyzed by One-Way ANOVA as $p \leq 0.05$ according to post hoc test (Tukey). The data had superscript (a) as no significant change.

1.4.Histopathological findings

Al₂O₃-NPs on rats' liver tissue reveals significant hepatotoxic effects, characterized by various pathological alterations as summarized briefly:

Group 1 (G1): serving the control group, which showed normal hepatic structure with normal hepatocytes with hexagonal shape arranged in rows, normal central vein and portal triad (Fig 3).

Group 2 (G2): Rats exposed to 15mg/kg Al₂O₃-NPs over a 60-day period demonstrated mild pathological changes in liver tissue of rats expressed by degeneration of the hepatocytes cytoplasm and nuclei and some of them disappeared (Fig 4).

While **group 3 (G3)** exposed to 30mg/kg Al₂O₃-NPs showed sever pathological changes in the hepatocytes; the lesions varied from mild degenerative changes represented by vacuolation and rarefication of cytoplasm with shrinkage of nuclei which may disappear. The necrobiotic changes were identified by nuclear and cytoplasmic changes, some nuclei were pyknotic and others were fragmented, lysed or disappeared. The cytoplasm was condensed and deeply stained with eosin in the apoptotic cells to marked rarefication and lysis with faint staining (Fig 5). The portal area showed infiltration with mononuclear cells, increased number of bile ductules and degeneration of hepatocytes (Fig 6).

The renal tissue of Al₂O₃-NPs treated groups showed different pathological alteration discussed in details;

Group 1 (G1): Serving as a control, this group exhibited normal kidney architecture with well-developed glomeruli and tubules (Fig 7).

Kidneys of rats treated with Al₂O₃-NPs (15mg/kg BW/60d), **Group 2 (G2)**; demonstrated focal interstitial nephritis explained by localized infiltration of mononuclear cells between renal tubules (fig 8). In **Group 3 (G3)**; treated with Al₂O₃-NPs (30mg/kg BW/60d), the Degenerative changes in the renal tubules included vacuolated cytoplasm with pyknotic nuclei, proliferation of fibroblasts and dilated vascular glomerular capillaries (Fig 9). Interstitial nephritis was apparent, with infiltration of mononuclear cells (Fig 10). The kidney also showed thickening of the glomerular basement membrane and exfoliated cells within the lumen (Fig 11). These findings highlight the nephrotoxic potential of Al₂O₃-NPs, as evidenced by inflammation and degeneration of renal tissues.

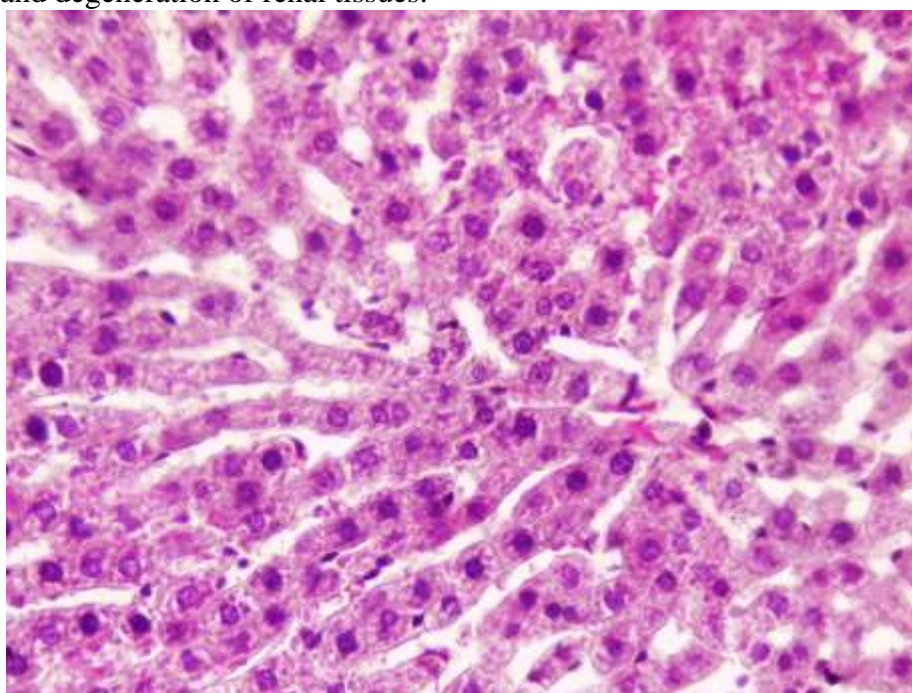


Fig 3: Histopathology of control rat's liver showing central vein with radiating hepatocytes.

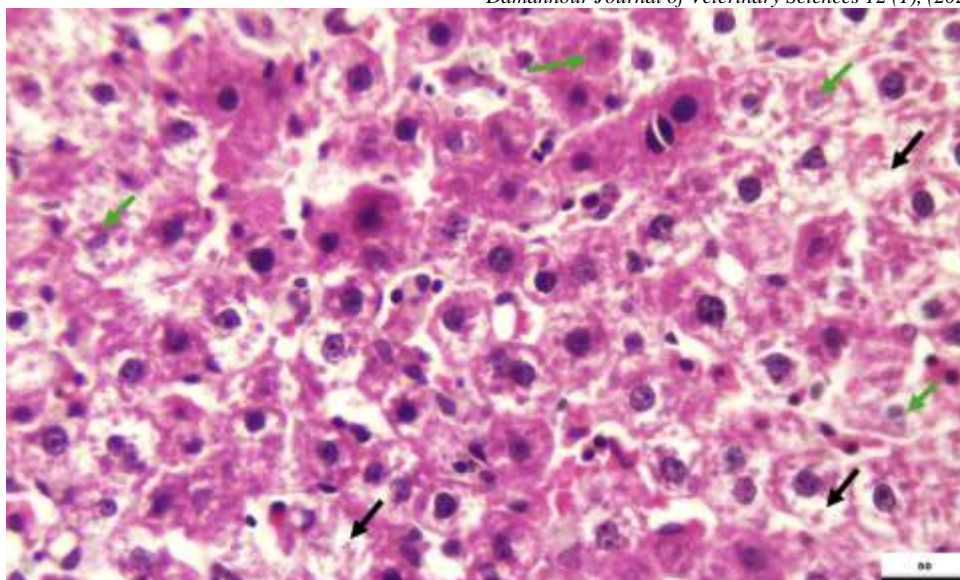


Fig 4: Histopathology of rat's liver exposed to (15mg/kg) Al_2O_3 -NPs showing vacuolated hepatocytes (black arrows) and other hepatocytes had degenerated nuclei leaving nuclear remnants (green arrows).

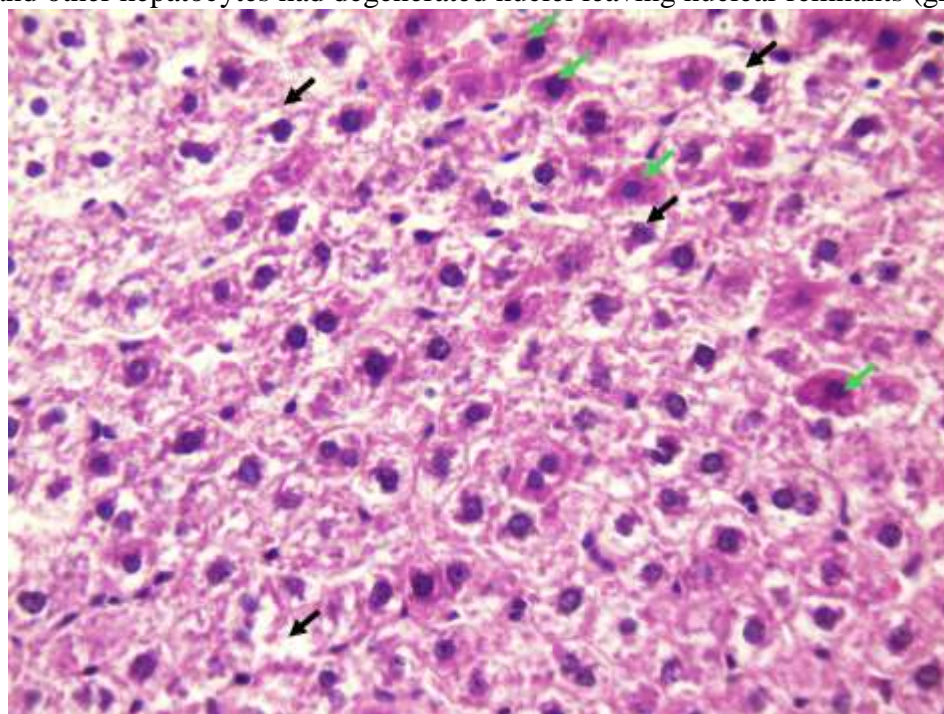


Fig 5: Histopathology of rat's liver exposed to (30mg/kg) Al_2O_3 -NPs showing area of massive vacuolation and degeneration as hepatocytes had pyknotic nuclei with eosinophilic cytoplasm (green arrows) and other cells had vacuolated cytoplasm (black arrows).

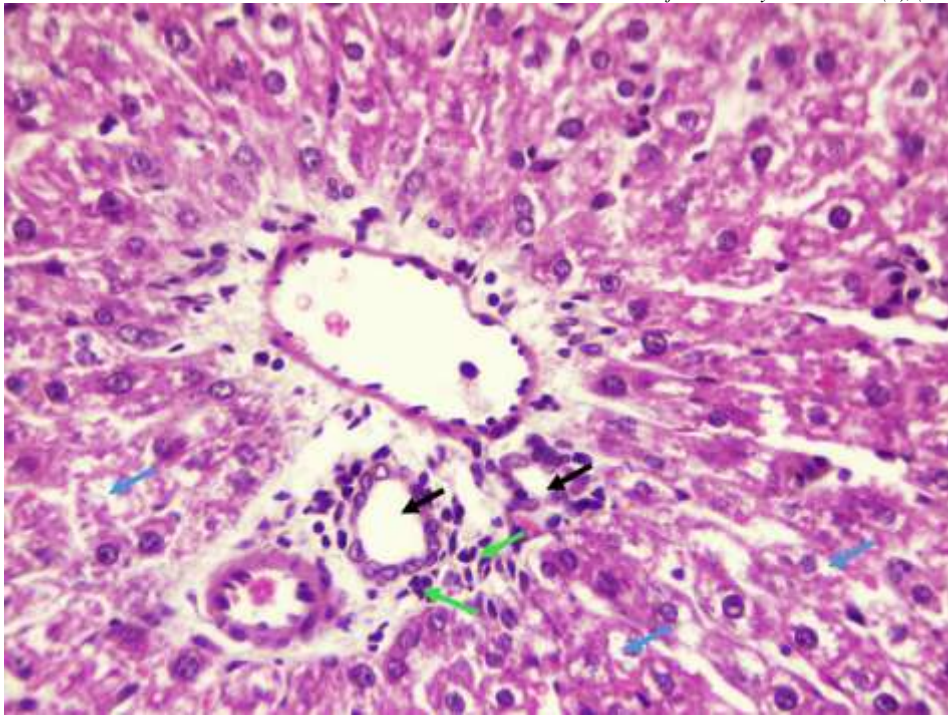


Fig 6: Histopathology of rat's liver exposed to (30mg/kg) Al_2O_3 -NPs showing portal area with mononuclear cells infiltration (green arrows), increased number of bile ductules (black arrows) and degenerated hepatocytes with degenerated nuclei or nuclear remnant (blue arrows).

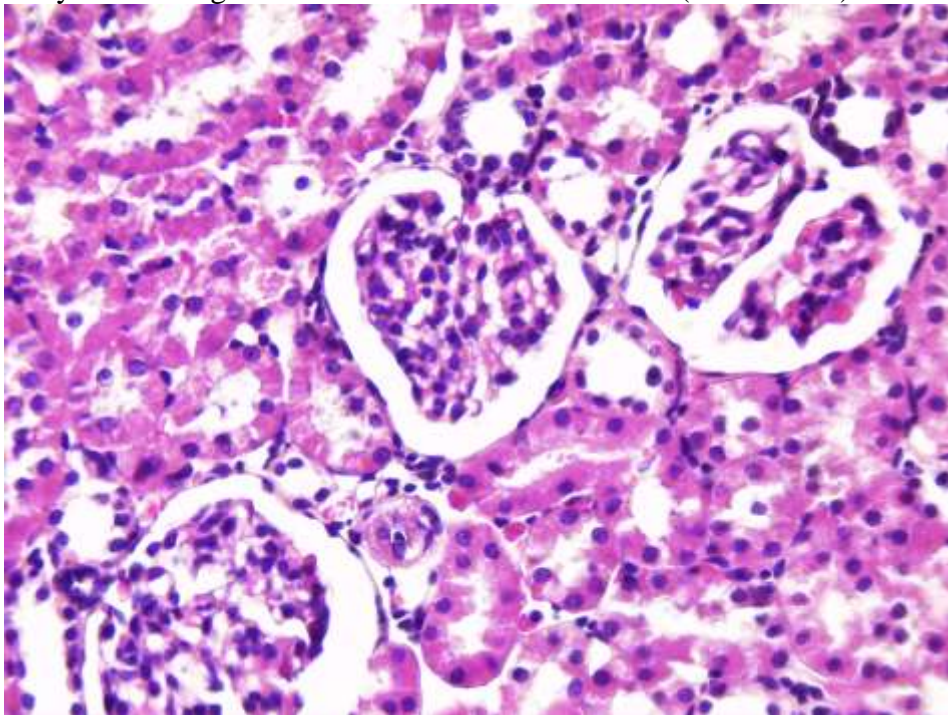


Fig 7: Histopathology of control rat's kidney showing normal renal glomeruli and renal tubules.

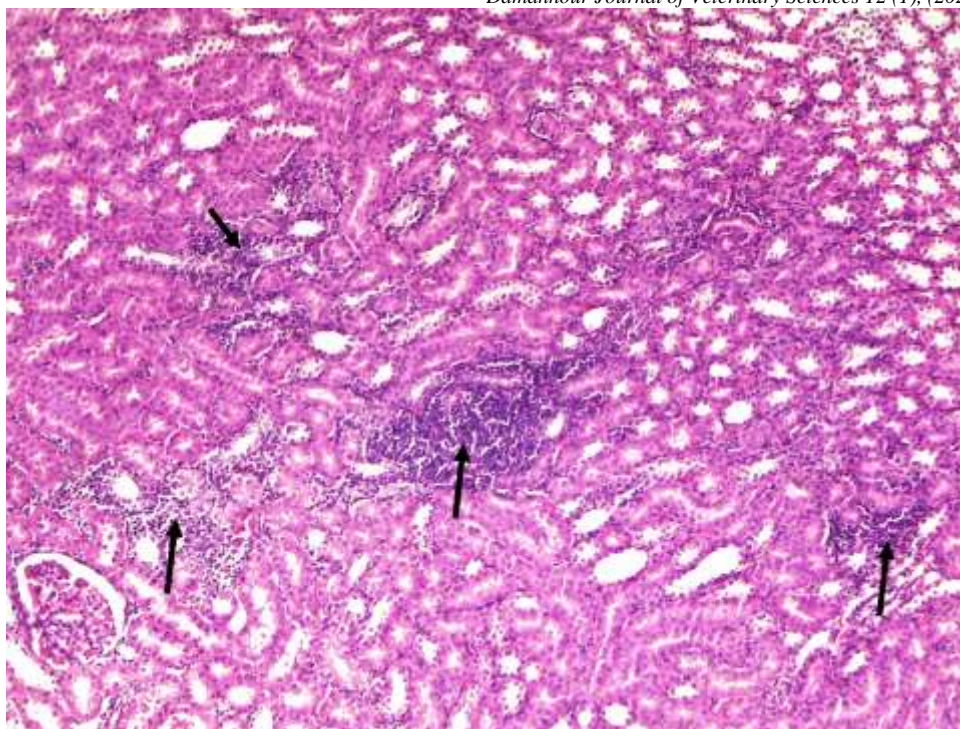


Fig 8: Histopathology of rat's kidney exposed to (15mg/kg) Al_2O_3 -NPs showing focal interstitial nephritis explained by mononuclear cells infiltration in the interstitial tissue (black arrows).

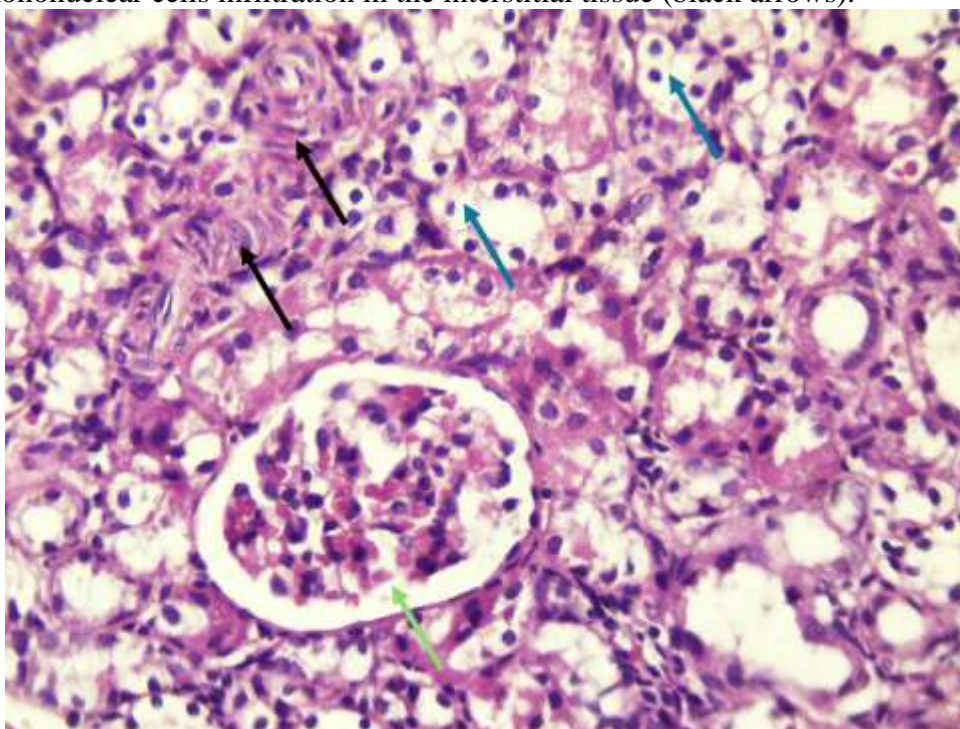


Fig 9: Histopathology of rat's kidney exposed to (30mg/kg) Al_2O_3 -NPs showing vacuolated cytoplasm with pyknotic nuclei in the renal tubular cells (blue arrows), proliferation of fibroblast cells (black arrows) and dilated vascular glomeruli (green arrow).

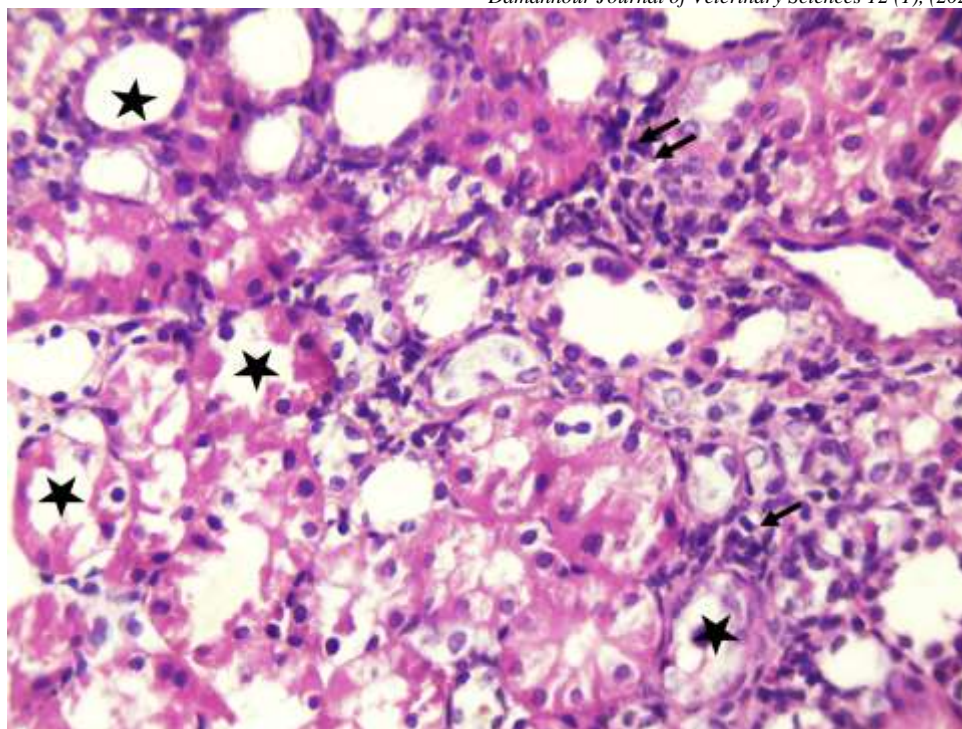


Fig 10: Histopathology of rat's kidney exposed to (30mg/kg) Al_2O_3 -NPs showing area of degeneration and necrosis of renal tubules (black stars) with interstitial nephritis represented by mononuclear cells infiltration (black arrows).

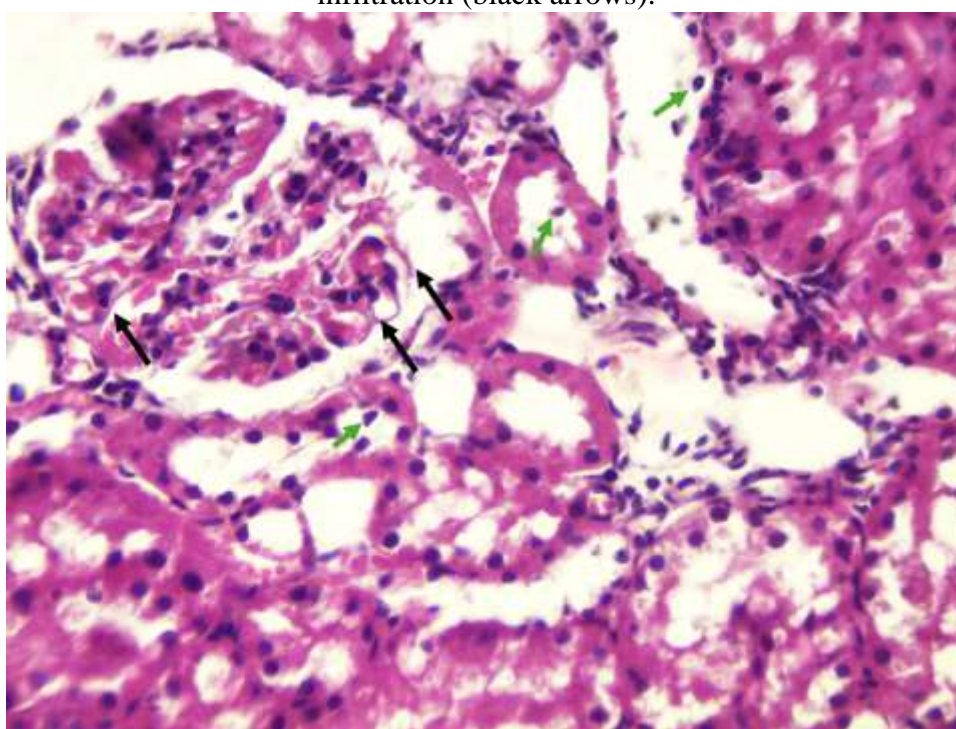


Fig 11: Histopathology of rat's kidney exposed to (30mg/kg) Al_2O_3 -NPs showing thickening of the glomerular basement membrane (black arrows) and exfoliated cells into the lumen of renal tubules (green arrows).

1.5.Oxidative markers assay

Al_2O_3 -NPs enhanced the oxidative stress injury in G2 and G3 as depicted in (Table 2 and fig 12). A noticeable increase in the MDA level was noted as compared to the NC.

| Group | Liver MDA | kidney MDA |
|---------|-------------------------|-------------------------|
| Control | 26±2.08 ^c | 23.33±2.03 ^c |
| Low AL | 67±2.09 ^b | 68.6±6.11 ^b |
| High AL | 78.83±7.16 ^a | 71.6±6.48 ^a |

Table (2): Data presented as Mean Values \pm SE (n=10) For each parameter in the different animal groups after 60d. The groups with different superscripts within the same row are significantly different at $P \leq 0.05$, one-way ANOVA with Tukey's HSD.

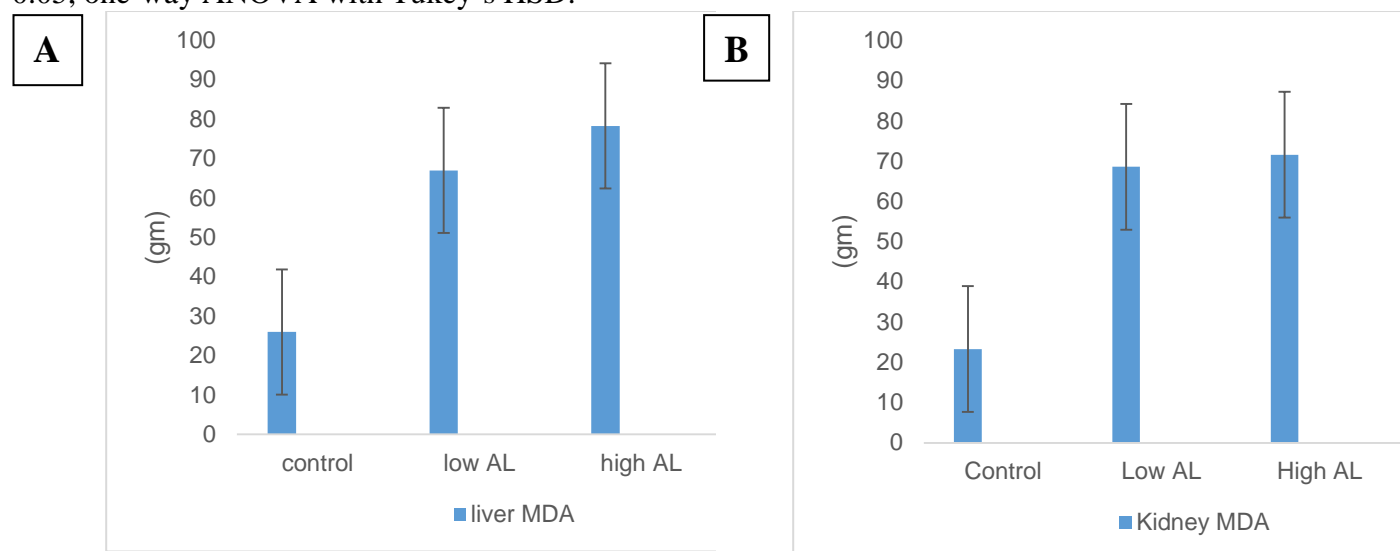


Fig 12: the effect of Al_2O_3 -NPs on the level of MDA as (A): showed an increase in the level of liver MDA in both Al_2O_3 -NPs treated groups. (B): showed an increase in the level of kidney MDA in both of Al_2O_3 -NPs treated groups. Values are expressed as mean values \pm SD and $P \leq 0.05$, one-way ANOVA with Tukey's HSD.

1. Discussion:

Exposure to metallic nanoparticles, particularly Al_2O_3 -NPs, is a growing concern due to their widespread application in industries such as cosmetics, food packaging, and pharmaceuticals. These nanoparticles can easily come into contact with humans, potentially leading to cellular oxidative stress (Yousef et al., 2022). Our research has highlighted the toxicity of Al_2O_3 -NPs, particularly their role in promoting oxidative stress and injury across various organs.

There was degeneration in hepatocytes and single cells necrosis with vacuolation in the liver of low Al_2O_3 -NPs treated groups and the pathological changes became more severe in the high Al_2O_3 -NPs treated group (Arpita De et al., 2020; Makwana et al., 2024). Such signs of degeneration, especially shrunken and pyknotic nuclei, therefore, suggest that Al_2O_3 -NPs induce some degree of cellular stress or insult. Pyknotic nuclei often suggest apoptotic or early necrotic changes; hence, these nanoparticles may disturb normal cellular function and trigger cell-death pathways. The localized damage further suggests that not all hepatocytes are equally sensitive to the action of nanoparticles, which may be related to different metabolic activities and receptor expressions. Large-scale necrosis of hepatocytes, cellular infiltrations, congestions of central veins, and blood sinusoids were induced by Al_2O_3 -NPs (Alghriany, Omar, Mahmoud, & Atia, 2022; M. I. Yousef, T. F. Mutar, & M. A. E. Kamel, 2019). In most

instances, vacuolation usually reflects a state of cellular dysfunction wherein the normal processes of detoxification and metabolism are impaired. The presence of necrosis further justifies the view of extensive liver damage, signaling that hepatocytes are not simply stressed but actually experience irreversible injury (Hamdi & Hassan, 2021). In line with the previous findings, the exposure to Al_2O_3 -NPs significantly reduced final body weight and weight gain compared to the control group. This observation is consistent with the study by Shumakova et al (Shumakova et al., 2015), which reported that the simultaneous administration of Al_2O_3 -NPs and Pb caused notable changes in relative body and organ weights.

The buildup of Al_2O_3 -NPs in the kidney tissues can significantly disrupt the oxidant and antioxidant mechanism, resulting in various noticeable pathological changes in kidney structure leading to cell injury and damage so the high Al_2O_3 -NPs dose cause more severe pathological changes than the low Al_2O_3 -NPs dose in compared with control group (Arpita De et al., 2020). The pathological alterations in kidneys tissues were evidenced by degenerative changes in the renal tubules included vacuolated cells with pyknotic nuclei and exfoliated nuclei within the lumen, interstitial nephritis was apparent, with infiltration of mononuclear cells and fibroblasts. Thickening of the glomerular basement membrane and dilated vascular glomeruli. Moreover, the pathological changes were in line with previous researchers who

proved toxic effect of Al₂O₃-NPs in various organs (Yousef et al., 2022).

One of the important mechanisms of tissue damage following exposure to NPs and ultrafine particles is oxidative stress (Bhabra et al., 2009). NPs can induce oxidative stress in cells through different pathways, the high reactivity of many NPs is capable of generating reactive oxygen species directly on their surfaces (Schraufnagel, 2020). In addition, these particles can also disrupt mitochondrial function, leading to increased levels of ROS (Bhabra et al., 2009). In the present study, according to the results of the experiment, rats exposed to 30 mg/kg BW of Al₂O₃-NPs for a period of 60 days exhibited significantly higher values of MDA than 15mg/kg of ROS compared to the control group. This was definitely referring to the toxic effect of Al₂O₃-NPs in the exaggeration of oxidative stress in the liver and kidney of rats. As MDA is considered the end product of lipid peroxidation and their increased quantity gives direct proof of noxious process caused by the free radical (Afifi, Saddick, & Zinada, 2016). Al₂O₃-NPs engage with proteins and nucleic acids inside the cell, disrupting normal cellular processes and contributing to oxidative stress. This interaction is vital as it triggers a series of cellular events that culminate in damage (Alshatwi et al., 2013; Elkhadrawy, Abou-Zeid, El-Borai, El-Sabbagh, & El-Bialy, 2021). In vitro, Al₂O₃-NPs showed dose-dependent cytotoxicity toward neuronal and bronchial cell types derived from different tissues. Their concentration determines their degree of toxicity, since higher doses kill more cells and induce observable morphological changes (Zhang, Xiong, & Liu, 2022). Significantly, it was found that Al₂O₃-NPs appeared more toxic, confirming again another form of nanoparticles being a factor in assessing its toxicity (Xuan, Ju, Skonieczna, Zhou, & Huang, 2023).

2. Conclusion:

Al₂O₃-NPs has been identified as contributors to renal and hepatic toxicity, particularly when used in a high concentration. Research suggests that these adverse effects are associated with several biological mechanisms, primarily involving oxidative stress and inflammation. Exposure to Al₂O₃-NPs results in increased levels of MDA which serves as an indicator of oxidative DNA damage and reflects heightened oxidative stress.

Overall, these observations evidence the high hepatorenal toxic potential of Al₂O₃-NPs. Degenerative changes, vascular congestion, and focal necrosis together indicate that exposure to these nanoparticles can result in impaired liver and kidney functions, thus raising serious concerns

about their applications, especially in medicine and industries.

References

- Abd-Elhakim, Y. M., Hashem, M. M., Abo-EL-Sooud, K., Hassan, B. A., Elbohi, K. M., & Al-Sagheer, A. A. (2021). Effects of co-exposure of nanoparticles and metals on different organisms: a review. *Toxics*, 9(11), 284.
- Afifi, M., Saddick, S., & Zinada, O. A. A. (2016). Toxicity of silver nanoparticles on the brain of *Oreochromis niloticus* and *Tilapia zillii*. *Saudi journal of biological sciences*, 23(6), 754-760.
- Alghriany, A. A. I., Omar, H. E. M., Mahmoud, A. M., & Atia, M. M. (2022). Assessment of the Toxicity of Aluminum Oxide and Its Nanoparticles in the Bone Marrow and Liver of Male Mice: Ameliorative Efficacy of Curcumin Nanoparticles. *ACS Omega*, 7(16), 13841-13852. doi:10.1021/acsomega.2c00195
- Alshatwi, A. A., Subbarayan, P. V., Ramesh, E., Al-Hazzani, A. A., Alsaif, M. A., & Alwarthan, A. A. (2013). Aluminium oxide nanoparticles induce mitochondrial-mediated oxidative stress and alter the expression of antioxidant enzymes in human mesenchymal stem cells. *Food Additives & Contaminants: Part A*, 30(1), 1-10.
- Awashra, M., & Młynarz, P. (2023). The toxicity of nanoparticles and their interaction with cells: an in vitro metabolomic perspective. *Nanoscale Advances*, 5(10), 2674-2723.
- Bhabra, G., Sood, A., Fisher, B., Cartwright, L., Saunders, M., Evans, W. H., . . . Davis, S. A. (2009). Nanoparticles can cause DNA damage across a cellular barrier. *Nature nanotechnology*, 4(12), 876-883.
- De, A., Ghosh, S., Chakrabarti, M., Ghosh, I., Banerjee, R., & Mukherjee, A. (2020). Effect of low-dose exposure of aluminium oxide nanoparticles in Swiss albino mice: Histopathological changes and oxidative damage. *Toxicol Ind Health*, 36(8), 567-579. doi:10.1177/0748233720936828
- De, A., Ghosh, S., Chakrabarti, M., Ghosh, I., Banerjee, R., & Mukherjee, A. (2020). Effect of low-dose exposure of aluminium oxide nanoparticles in Swiss albino mice: Histopathological changes and oxidative damage. *Toxicology and Industrial Health*, 36(8), 567-579.

- Draper, H. H., & Hadley, M. (1990). [43] Malondialdehyde determination as index of lipid Peroxidation *Methods in enzymology* (Vol. 186, pp. 421-431): Elsevier.
- Elkhadrawy, B., Abou-Zeid, S., El-Borai, N., El-Sabbagh, H., & El-Bialy, B. E.-S. (2021). Potential toxic effects of aluminum nanoparticles: an overview. *Journal of Current Veterinary Research*, 3(2), 94-106.
- Hamdi, H., & Hassan, M. M. (2021). Maternal and developmental toxicity induced by Nanoalumina administration in albino rats and the potential preventive role of the pumpkin seed oil. *Saudi J Biol Sci*, 28(8), 4778-4785. doi:10.1016/j.sjbs.2021.05.003
- Kalashnikova, I., Chung, S.-J., Nafiujjaman, M., Hill, M. L., Siziba, M. E., Contag, C. H., & Kim, T. (2020). Ceria-based nanotheranostic agent for rheumatoid arthritis. *Theranostics*, 10(26), 11863.
- Kumah, E. A., Fopa, R. D., Harati, S., Boadu, P., Zohoori, F. V., & Pak, T. (2023). Human and environmental impacts of nanoparticles: a scoping review of the current literature. *BMC Public Health*, 23(1), 1059.
- Lee, S. H., & Jun, B.-H. (2019). Silver nanoparticles: synthesis and application for nanomedicine. *International journal of molecular sciences*, 20(4), 865.
- Li, B., & Tang, M. (2020). Research progress of nanoparticle toxicity signaling pathway. *Life Sciences*, 263, 118542.
- Makwana, A. A., Fefar, D. T., Delvadiya, R. S., Thakore, K. A., Patel, S. S., Patel, U. D., . . . Gajera, K. G. (2024). Hepato-toxic effects of aluminium oxide nanoparticles following repeated dose 28-day oral exposure in Wistar rats.
- Murrell, K. D., Leighton, E. A., Boswell, B. A., & Gasbarre, L. C. (1989). Comparison of egg excretion and serum pepsinogen levels as measures of nematode worm burdens in calves with limited pasture exposure. *The Journal of Parasitology*, 360-366.
- Rashki, S., Asgarpour, K., Tarahimofrad, H., Hashemipour, M., Ebrahimi, M. S., Fathizadeh, H., . . . Salavati-Niasari, M. (2021). Chitosan-based nanoparticles against bacterial infections. *Carbohydrate polymers*, 251, 117108.
- Saratale, R. G., Saratale, G. D., Shin, H. S., Jacob, J. M., Pugazhendhi, A., Bhaisare, M., & Kumar, G. (2018). New insights on the green synthesis of metallic nanoparticles using plant and waste biomaterials: current knowledge, their agricultural and environmental applications. *Environmental Science and Pollution Research*, 25, 10164-10183.
- Schraufnagel, D. E. (2020). The health effects of ultrafine particles. *Experimental & molecular medicine*, 52(3), 311-317.
- Shin, T. H., Lee, H.-S., Park, H. J., Jin, M. S., Paik, M.-J., Manavalan, B., . . . Lee, G. (2018). Integration of metabolomics and transcriptomics in nanotoxicity studies. *BMB reports*, 51(1), 14.
- Shumakova, A., Trushina, E., Mustafina, O., SKh, S., Gmoshinsky, I., & Khotimchenko, S. (2015). Lead toxicity in its joint administration with the aluminium oxide nanoparticles to rats. *Voprosy pitaniia*, 84(3), 40-49.
- Suvarna, K. S., Layton, C., & Bancroft, J. D. (2018). *Bancroft's theory and practice of histological techniques*: Elsevier health sciences.
- Wagner, A. J., Bleckmann, C. A., Murdock, R. C., Schrand, A. M., Schlager, J. J., & Hussain, S. M. (2007). Cellular interaction of different forms of aluminum nanoparticles in rat alveolar macrophages. *The journal of physical chemistry B*, 111(25), 7353-7359.
- Xuan, L., Ju, Z., Skonieczna, M., Zhou, P., & Huang, R. (2023). Nanoparticles-induced potential toxicity on human health: Applications, toxicity mechanisms, and evaluation models. *MedComm*, 4 (4), e327.
- Yousef, M. I., Mutar, T. F., & Kamel, M. A. E. (2019). Hepato-renal toxicity of oral sub-chronic exposure to aluminum oxide and/or zinc oxide nanoparticles in rats. *Toxicol Rep*, 6, 336-346. doi:10.1016/j.toxrep.2019.04.003
- Yousef, M. I., Roychoudhury, S., Jafaar, K. S., Slama, P., Kesari, K. K., & Kamel, M. A. E.-N. (2022). Aluminum oxide and zinc oxide induced nanotoxicity in rat brain, heart, and lung. *Physiological research*, 71(5), 677.
- Zhang, N., Xiong, G., & Liu, Z. (2022). Toxicity of metal-based nanoparticles: challenges in the nano era. *Front. Bioeng. Biotechnol.* 2022. 10: 1001572.